RECONSTRUCTION OF BUILDING MODELS WITH ROOF PATCH CLASSIFICATION

Yun-Jou Lin [*a] and Liang-Chien Chen [b]

[*a] Research assistant, Central for Space and Remote Sensing Research, National Central University
300 Jhongda Rd., Jhongli, Taoyuan 32001, Taiwan; Tel: +886-3-4227151#57623
Email: 100322079@cc.ncu.edu.tw
[b] Professor, Central for Space and Remote Sensing Research, National Central University,
300, Jhongda Rd., Jhongli, Taoyuan 32001, Taiwan; Tel: + 886-3-4227151#57622;
E-mail: lcchen@csrsr.ncu.edu.tw

KEY WORDS: Lidar Data,Aerial Imagery, Roof Patch Classification, Reconstruction

Abstract: Building models are indispensable for the representation of the real world in 3D geographic information systems. The proposed paper combines the distinct edges from aerial imagery and accurate elevation from lidar data to reconstruct the building models. Most of the man-made buildings are constructed with planes and straight lines so this paper aims at the plane roofs.
First, the lidar point clouds on the roof are extracted to form the roof patches. The connectivity among the roof patches is analyzed. We classify the roof planes to three types, namely, flat roof patches, mono-pitched roof patches and multi-pitched roof patches. The roof structure lines exist in the multi-pitched roof patches. Therefore, we detect the zone of roof structure lines and the boundaries of three different roof patches are tracked in the object space. The zone of roof structure lines and the initial boundaries are projected to the imagery for buffering the zones of structure lines. Next, we detect the edges with Canny detector in the work area and vectorization for each edge, the line segments are projected to object space to reconstruct 3D building models with SMS(Split-Merge-Shape). Finally, the height of building models are adjusted with lidar point clouds to determine the accurate height.
The experimental cases include different kinds of roof planes. The proposed method is validated using manually measured 3D building models as reference data. The test data include (1) DMC aerial imagery with a spatial resolution of 17cm, and (2) lidar point clouds from Leica ALS 50 with a spatial resolution of 10 points/m^2. The experimental results indicate that the reconstruction may reach high accuracy and with high degree of automation.

1. INTRODUCTION

In the geospatial information systems, building reconstruction is an important task to describe the three dimensional world for many application, such as urban planning and management, disaster prevention and other decision support. In building modeling, the available multi-sources contain remote sensing data and digital maps, which are general available and show clear building boundaries. The combination of the digital maps and other sources for building modeling facilitate the location of building areas and provide precise boundaries (Suveg and Vosselman, 2004). However, digital maps have insufficient temporal resolution. Therefore, we used the remote sensing sources for this study.

In remote sensing resources, aerial imagery and lidar data are used frequently in building modeling. Aerial imagery has high horizontal resolution and high overlap and is commonly available at a low cost. Many studies have focused on stereo images and multiple images matching for reconstruction (Kim and Nevatia, 2004). Nevertheless, the periodical texture in the building can easily occur incorrect matching (Ok et al., 2010). On the other hand, the lidar data can provide the plentiful surface information and accurate elevation. The edge in the lidar data are vague so some geometric constrains are added to generate the building boundaries (Sampath and Shan, 2010). Brenner (2005) proposed the combination between lidar data and aerial imagery can increase the quality and automation in building reconstruction.

This paper uses the complementary data, aerial imagery and lidar data, to reconstruct the building models. The proposed scheme comprises five major parts, (1) segmentation of roof patches, (2) roof patches classification, (3) determination of structure lines, (4) 2D line segmentation, and (5) reconstruction. First, the lidar point clouds on the roof are extracted to form the roof planes and the points on the roofs are segmented to roof patches. Then, the roof patches are classified to three different types, namely, flat roof patches, mono-pitched roof patches and multi-pitched roof patches, by analyzing the slopes of patches and the connectivity between the patches. The roof structure lines exist in the multi-pitched roof patches. Therefore, we detect the zone of roof structure lines and the boundaries of three different roof patches are tracked in the object space. The zone of roof structure lines and the initial boundaries are projected to the imagery for buffering the zones of structure lines. Then, the initial boundaries are back projected to imagery for determining the precise edges. In the next step, the edges from the imagery are vectorized to generate the line segments and projected to object space to reconstruct the 3D building models. Finally, the height of building models are adjusted with lidar point clouds to determine the accurate height.

2. METHODOLOGYS

The proposed scheme is composed of five major parts, (1) Segmentation of Roof Patches, (2) Roof Patch Classification, (3) Determination of Structure Lines, (4) 2D Line Segmentation, and (5) Reconstruction. The flowchart of proposed method is shown in Figure1.

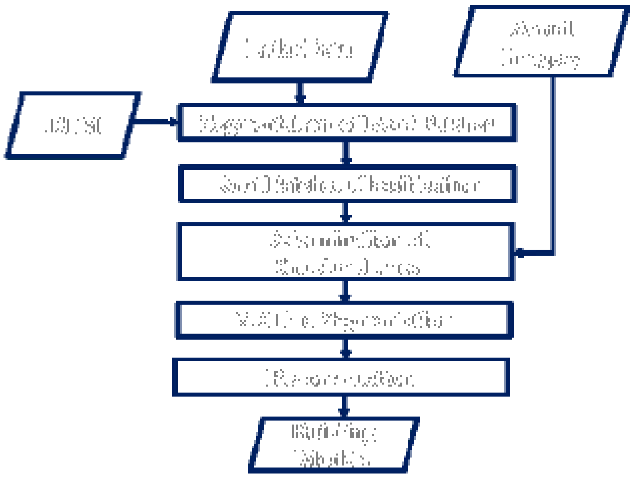

Figure 1: Flowchart of proposed method

Segmentation of Roof Patches

The roof patches are generated from the lidar point clouds. We extracted the roof point clouds by eliminating lidar points on the walls and grounds. The heights of lidar point clouds are subtracted from the terrain elevations in the DEM to derive the normalized height. Then, the TIN structure is constructed with the lidar point clouds to remove the lidar point clouds on the walls and grounds. Then, the local surfaces are generated with the cylinder model (Filin and Pfeifer, 2005). The region growing is applied to the local surfaces to derive the roof patches. We separate the roof patches with different slopes into potential flat roof patches and pitched roof patches. The roof patches are separated by judging the included angles between the vertical direction roof patches.

Roof Patch Classification

From the previous step, we separate the roof planes into two main types, flat roof patches and pitched roof patches. The roof patches are categorized as pitched roof patches and potential flat roof patches. The high pitched roof patches are easy to be segmented in the first step. However, potential flat roof patches may consist of flat roof patches or low pitched roof patches. Therefore, in this part, the potential flat roofs are validated. After determining all the roof patches. The roof patches are classified to flat, multi-pitched and mono-pitched roof patches with connectivity analysis.

In the connectivity analysis, the connective relation between the pitched roof patches was determined. The pitched roof patches were separated into multi-pitched roof patches and mono-pitched roof patches. The multi-pitched roof patches consist of two or more patches. The two connected pitched roof patches can be determined from the common point clouds. The mutual connected roof patches were grouped into a region for boundaries determination.

Determination of Structure Lines

In the structure lines determination, the initial boundaries and the roof structure zones are decided. The structure lines contain the roof structure lines and building boundaries. In the boundaries part, we project the lidar point clouds to the 2D grid plane to trace the boundary. The method of boundary tracing is shown in Figure 2. In the roof structure lines part, we determine the zones of roof structure lines from the connected pitched roof patches. Then, the zones are used to decide the roof structure lines in the imagery.

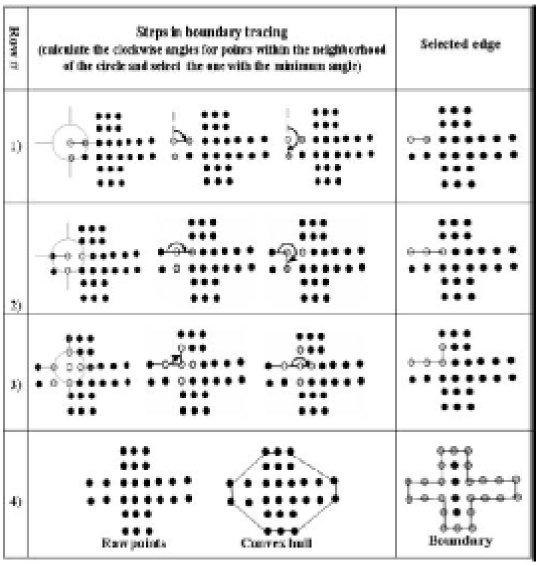

Figure 2: Boundary tracing (Sampath and Shan, 2007)

2D Line Segmentation

In the 2D line segments generation, we determine the precise line segments from the edges in the imagery. From the previous steps, the location of every structure lines is found. Hence, we used the precise line segments in the imagery as the structure lines.

We project the initial boundaries and the zones of the roof structure lines to the imagery to locate the precise lines. In the buffers of structure lines, the Canny operator (Canny, 1986) is used to detected the line structures. Then the edges are transformed to straight feature lines via Hough transformation (Hough, 1962).

Reconstruction

In the 3D building models reconstruction, 3D line segments are shaped to generate roof polygons, and heights of polygons are modified with lidar point clouds. After projecting the line segments to the object space, the line segments are reconstructed to the model with SMS algorithm. The heights of projected line segments are approximations so we modify the reconstructed models with the lidar point clouds using RANSAC.

3. EXPERIMENTAL RESULTS

The data were obtained from DMC images and ALS 50 point clouds in the test. The resolution of the aerial image is 17cm and the average of LIDAR points is $10pt/m^2$. The different sources of case 1 are shown in Figure 3. The different sources of case 2 are shown in Figure 4.

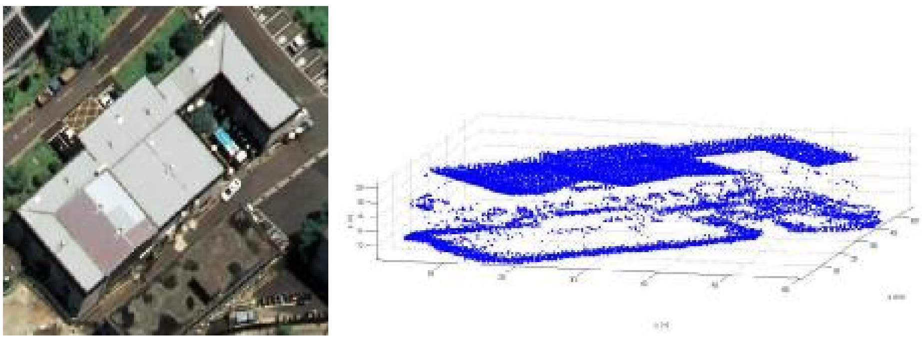

Figure 3 : Aerial Imagery and Lidar data in Case1

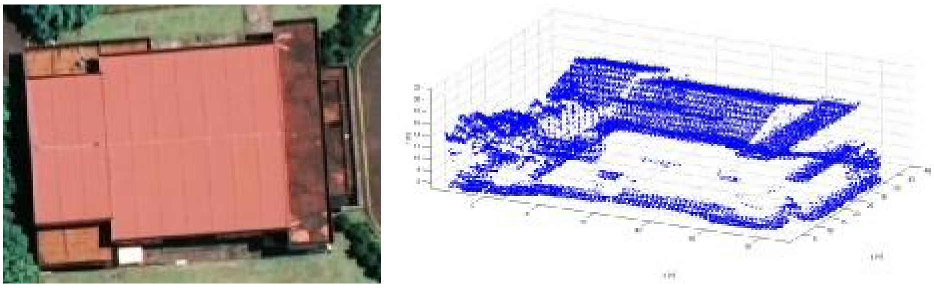

Figure 4 : Aerial Imagery and Lidar data in Case2.

In the first part the lidar point clouds are constructed to the TIN and the point clouds on the walls and grounds are removed. The TIN structures are shown in Figure 5. The TIN structure without the point clouds on the walls and grounds are shown in Figure 6. Then, we use the ldiar points on the roof to generate roof patches. The roof patches are shown in Figure 7.

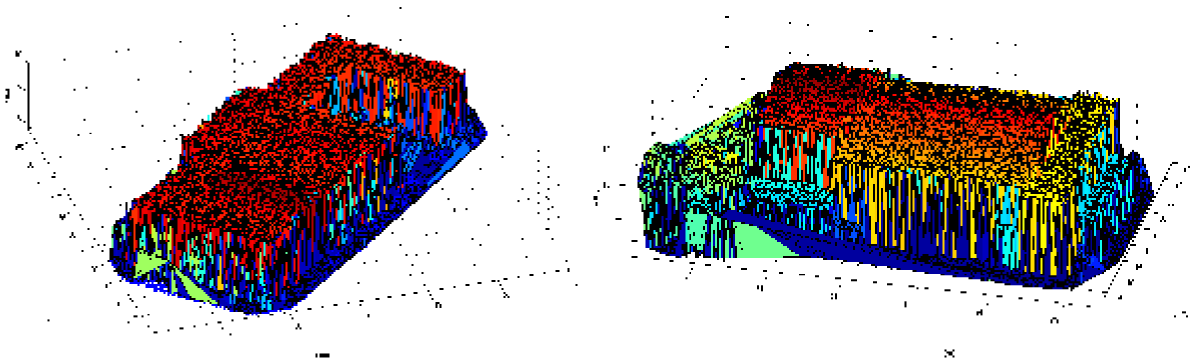

(a) (b)

Figure 5 : TIN structure
(a) Case 1, (b) Case 2

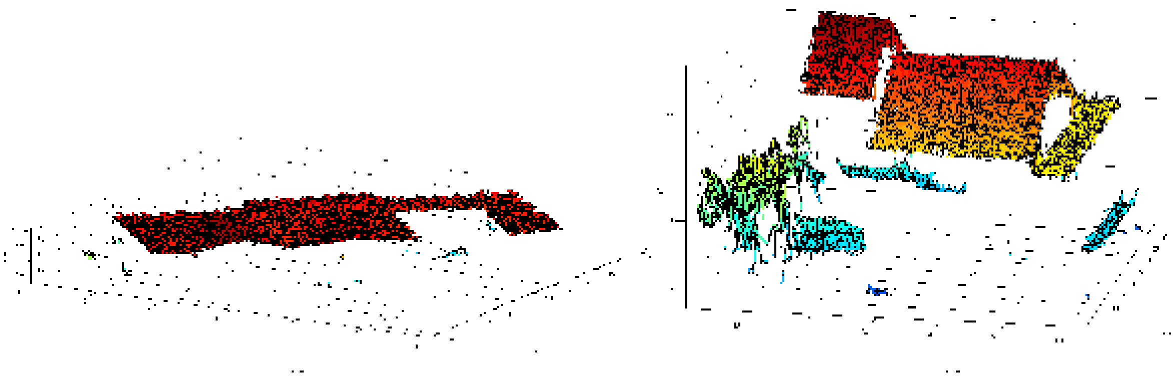

(a) (b)

Figure 6 : TIN structure without the point clouds on the walls and grounds
(a) Case 1, (b) Case 2

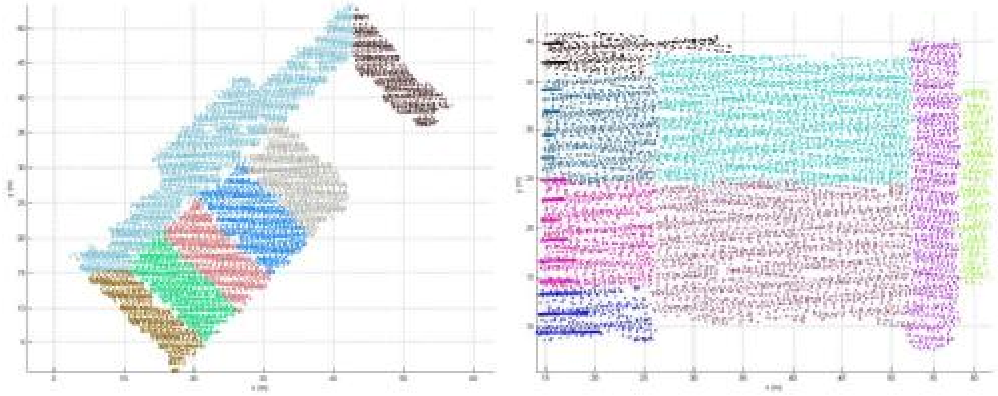

(a) (b)

Figure 7 : Roof Patch Segmentation
(a) Case 1, (b) Case 2

The initial boundaries and the zone of roof structure are projected to the imagery for locating the precise lines in the imagery. The line segments from the imagery are projected to the object space to generate the 3D line segments and then the 3D line segments are used to reconstruct the building models. The results of the building models in two cases are shown in Figure 8, respectively.

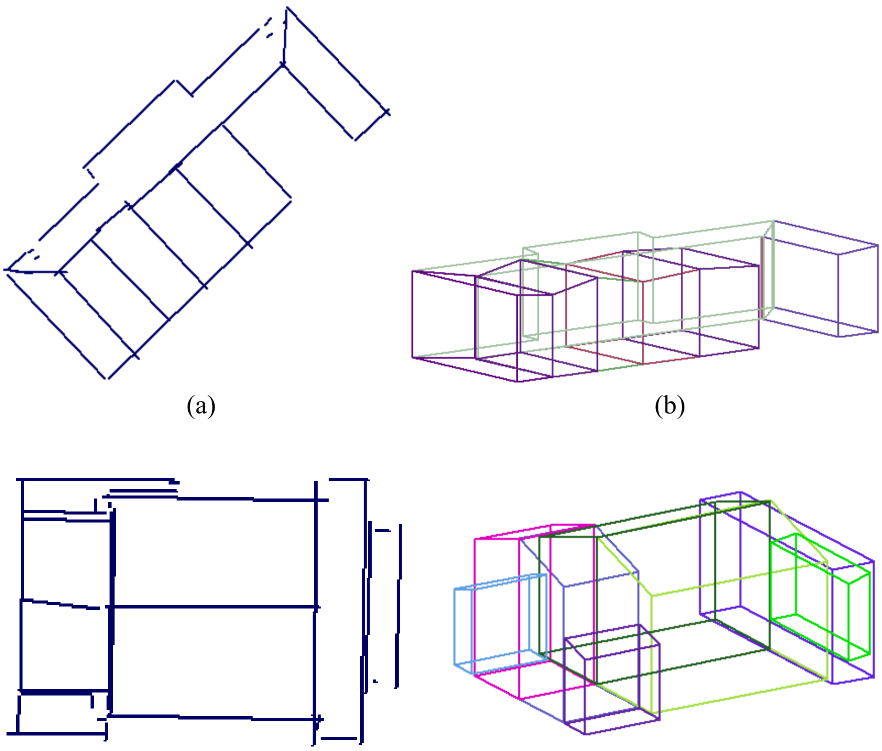

(a) (b)

(c) (e)

Figure 8 : Three dimensional line segments and building models
(a) Top view of 3D line segments in Case1 (b) Building models in Case1
(c) Top view of 3D line segments in Case2 (b) Building models in Case2

After reconstructing the building models, we can get the generated 3D coordinates. The RMSEs of the corners can be obtained from comparing the generated 3D coordinates and the stereo measurement of 3D building models. The RMSEs of the building corners are shown in Table 1. In the case 2, there were some minute line segments in the boundaries that could not be obtained in the line segments generation. Therefore, some of models in this part are incomplete.

Table 1 : RMSEs of building corners in object space

	$RMSE_X$ (m)	$RMSE_Y$ (m)	$RMSE_Z$ (m)	Number of corners
Case1	0.289	0.277	0.396	21
Case2	0.238	0.231	0.277	20

4. CONCLUSIONS

The proposed method integrated the lidar point clouds and aerial imagery to reconstruct the 3D building models. Based on the complementary characteristics of the obvious edges in the aerial imagery and accurate elevations in the lidar point clouds, we could reach quality 3D models. Compared with the manually measured models the experimental results indicated that the accuracy of the 3D coordinates direction could achieve an accuracy under 0.3m in the horizontal and in an accuracy under 0.4m in vertical direction. Since the target of this research is the buildings with planar facets, the proposed method is only applicable to polyhedral buildings.

REFERENCES:

Brenner, C., 2005, Building reconstruction from images and laser scanning. Int. J. Appl. Earth Obs. Geoinf., vol. 6, no. 3/4, pp. 187–198.

Canny, J., 1986, A Computational Approach to Edge Detection, IEEE Transactions on Pattern Analysis and Machine Intelligence, 8(6), pp. 679-698.

Filin, S. and Pfeifer, N., 2005, Neighborhood systems for airborne laser data. Photogrammetric Engineering and Remote Sensing, 71, pp. 743-755.

Hough, P.V.C., 1962, Methods and Means for Recognizing Complex Patterns. U.S. patent No. 3069654.

Kim, Z., and Nevatia, R., 2004, Automatic description of complex buildings from multiple images. Computer Vision and Image Understanding, 96 (1), pp. 60-95.

Ok, A.O., Wegner, J.D., Heipke, C., Rottensteiner, F., Soergel, U., and Toprak, V., 2010, A Stereo Line Matching Technique For Aerial Images Based on A Pair-Wise Relation Approach, International Archives of Photogrammetry and Remote Sensing, 38(1/W17), Istanbul (on CD-ROM).

Sampath, A. and Shan, J., 2007. Building boundary tracing and regularization from airborne LiDAR point clouds. Photogrammetric Engineering & Remote Sensing, 73 (7), pp. 805–812.

Sampath, A., Shan, J., 2010. Segmentation and reconstruction of polyhedral building roofs from aerial LiDAR point clouds. IEEE Transactions on Geoscience and Remote Sensing, 48 (3), pp. 1554–1567.

Suveg, I., Vosselman, G., 2004. Reconstruction of 3D building models from aerial images and maps. ISPRS Jornal Photogrammetry Remote Sensing, 58, 202–224.